CHAPTER 7

Electro-optical properties of a few binary mixtures of chiral rod-like and achiral hockey stick-shaped molecules

7.1. Introduction

Since the remarkable discovery of polar switching in achiral bent-core or banana-shaped compounds by Niori *et al*. [1], this class of mesogens has emerged as a field of considerable interest in liquid crystal research. Such a strong interest results from the exclusive structure-induced mesomorphic behavior and the exotic mesophase sequences revealed by the so-called banana-shaped compounds [2–4]. Notably, the structural uniqueness of the banana molecules (i.e., presence of a structural bend at the molecular core between the two flexible side chains) causes a spontaneous breaking of mirror symmetry and thereby leads to the formation of several exceptional columnar and smectic modifications with ferro-, antiferro- or ferrielectric properties and even unique chiral mesophase morphologies [1–10]. Such exceptional findings, including the observation of giant flexoelectricity [11, 12], unprecedented behavior of electroconvection patterns [13–15], a considerable Kerr effect [16], unique rheological properties [17, 18] in such mesogenic compounds has had a tremendous impact on the general field of soft condensed matter research.

It has also been observed that a trivial modification in conformation or structural composition or an alteration in the bend angle in such molecules can dramatically modify the phase-characteristics of the associated bent mesogens

and can even induce calamitic-like mesomorphism including nematic and layered smectics in them [19–22]. An intriguing example of such modulated structure is the hockey stick-shaped liquid crystals (LCs), where the lateral moieties attached to the central core, are asymmetrically configured on either sides of it, i.e., they possess a molecular shape, somewhat intermediate between the traditional rod-like and banana-shaped molecules. Such compounds are again much attractive in the sense that they can demonstrate a variety of atypical combinations of features pertaining to the fields of both symmetric bent-core and calamitic LCs. Moreover, the polar character of such compounds in calamitic-like Sm-*C* phases still remains not properly been understood. For a number of hockey stick-shaped mesogens, no feasible polar answer could be extracted from electro-optical measurements [23, 24]. However, there are also contradictory evidences of low, but clearly measurable spontaneous polarization in freestanding films formed by hockey stick-shaped liquid crystals [25]. Hence, it is of significant interest to study the resultant polar behavior from suitably prepared binary mixtures of hockey stick-shaped compounds with chiral rod-like liquid crystals.

In this chapter, the results on electro-optical measurements of a few binary liquid crystal mixtures consisting of the hockey stick-shaped 4-(3-*n*-decyloxy-2-methyl-phenyliminomethyl)phenyl 4-*n*-dodecyloxycinnamate and the antiferroelectric liquid crystal, (S)-MHPOBC have been described. Temperature dependences of spontaneous polarization, relaxation time, effective torsional viscosity and anchoring energy coefficients of the formulated mixtures have been investigated. The underlying aspects of the mutual interactions between the hockey stick-shaped and chiral mesogenic molecules and hence, the resultant modification in chiral environment of the host mesogenic medium has also been discussed.

7.2. Materials

The hockey stick-shaped liquid crystal, used for formulation of the mixtures, belongs to the homologues series of laterally methyl substituted, 4-(3-*n*-alkyloxy-2-methyl-phenyliminomethyl)phenyl 4-*n*-alkyloxycinnamates with m = 12, n = 10 (compound **5** as described in chapter 4). The antiferroelectric compound (S)-4-(1-methyl-heptyloxy carbonyl) phenyl 4′-octyloxybiphenyl-4-carboxylate (MHPOBC) was procured from Sigma Aldrich, USA (having purity higher than 99%) and has been used without further purification. The structural formulae and mesophase behavior of both the compounds (transition temperatures for MHPOBC are taken from Ref. [26]) are illustrated in figure 7.1.

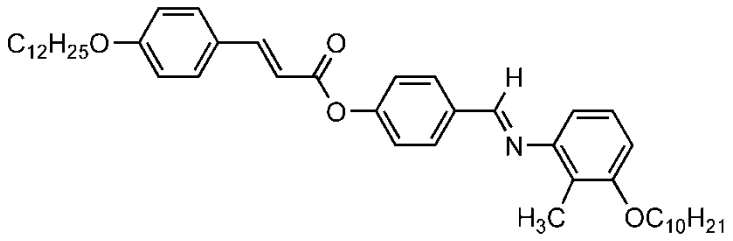

Cr 74.2 °C Sm-C_a 101.4 °C Sm-C_s 109.8 °C N 110.1 °C I

(a)

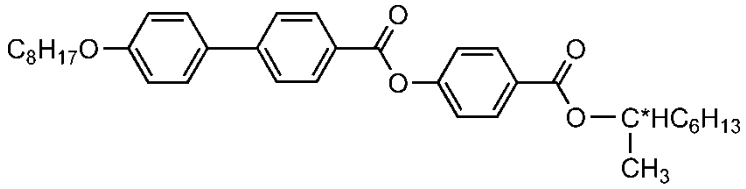

Cr 30 °C Sm-I_A* 66.0 °C Sm-C_A* 118.3 °C Sm-C_γ* 119.0 °C Sm-C_β* 120.7 °C Sm-C_α* 122.0 °C Sm-A 156 °C I

(b)

Figure 7.1. The chemical structure and phase behavior of (a) the hockey stick-shaped compound (compound **5**) and (b) the antiferroelectric calamitic compound [(S)-MHPOBC].

Four mixtures have been prepared with molar concentrations of the hockey stick-shaped compound ($x_{comp.5}$) equal to 0.1, 0.2, 0.4 and 0.5. The phase behavior of the mixtures and phase transition temperatures were identified by studying the temperature dependant variation of microscopic sample texture under a polarizing optical microscope (Motic BA 300) equipped with a Mettler FP900 hot stage and also from the polarization reversal current response.

7.3. Texture observation

The phase sequence and related phase transition temperatures of the four chiral-achiral mixtures consisting of hockey stick-shaped molecules are shown in figure 7.2. Upon cooling from the isotropic (*I*) phase, all the mixtures exhibit the following stable mesophase sequence, *I*–Sm-*A*–Sm-*C**–Sm-C_A*–*Cr*. However, the Sm-I_A* phase could not be resolved in the present study both from polarizing optical microscopy and spontaneous polarization measurements.

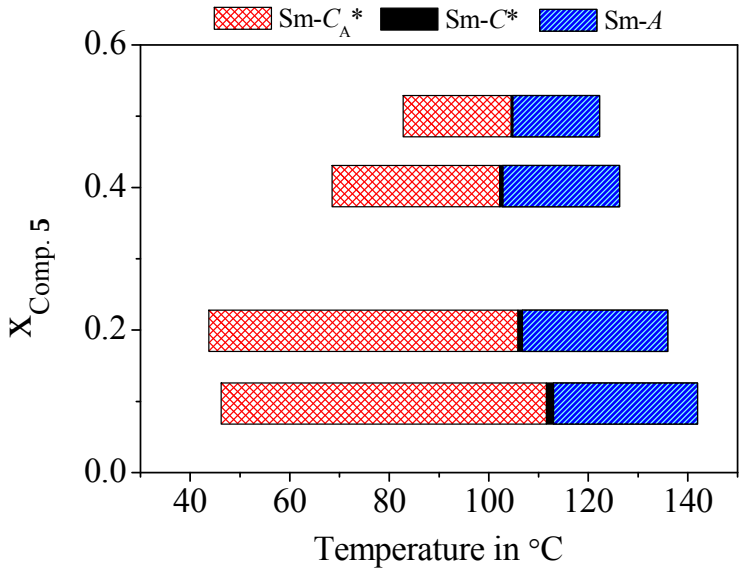

Figure 7.2. Phase transition temperatures of the binary mixtures comprising the hockey stick-shaped compound **5** and the antiferroelectric (S)-MHPOBC. The transition temperatures correspond to those obtained from polarizing optical microscopy and spontaneous polarization measurements.

The clearing temperature (T_{NI}) of all the mixtures were found to be lower than that of the pure (S)-MHPOBC and decreases linearly with increase in concentration of the achiral hockey stick-shaped compound, following the additive rule of mixture.

The characteristic photographs in different mesophases of one of the mixtures with concentration $x_{\text{comp.5}} = 0.1$ from polarizing optical microscopy (POM), are illustrated in figures 7.3(a)–(e). Upon cooling from the isotropic phase, just below the transition, a bâtonnets-shaped texture, characteristic of Sm-*A* phase appears [figure 7.3(a)]. With lowering of temperature, the bâtonnets grow anisotropically and then coalesce to form a fan-shaped texture of Sm-*A* phase [figure 7.3(b)]. From Sm-*A* phase the transition to the low temperature Sm-*C** phase is accompanied by a very little or almost no change in optical texture [figure 7.3(c)]. Therefore, the observations from spontaneous polarization measurements were also considered in ascertaining the Sm-*A*–Sm-*C** phase transition temperatures of all the mixtures under investigation. In two of the mixtures with lower concentration of the hockey stick-shaped compound, i.e., $x_{\text{comp.5}} = 0.1$and 0.2, the Sm-*A* widths are found to be close to one another and also to that observed in pure (S)-MHPOBC. However, considerable decrease has been observed in the other two mixtures having higher proportions of the hockey stick-shaped molecules, indicating a significant destabilization of the Sm-*A* phase in these mixtures.

The transition into the low temperature Sm-C_A*phase is accompanied by a distinctly observable change in the optical textures. The fan-shaped texture of the Sm-*C** phase was found to be transformed into the Sm-C_A* modification of a fan-shaped texture with irregular stripes across the fans [figure 7.3(d) and (e)]. Similar to the pure chiral component, in all the investigated mixtures, the antiferroelectric Sm-C_A* phase was found to be the dominant one over the mesophases sequence, always possessing the maximum width compared to the other smectic modifications. Nevertheless, the Sm-C_A*

range also suffers a substantial decrease for mixtures having greater share of the achiral mesogenic compound ($x_{\text{comp.5}} \geq 0.4$), indicating a significant influence of the hockey stick-shaped molecules on the packing arrangement and hence the phase-structure of the investigated binary system.

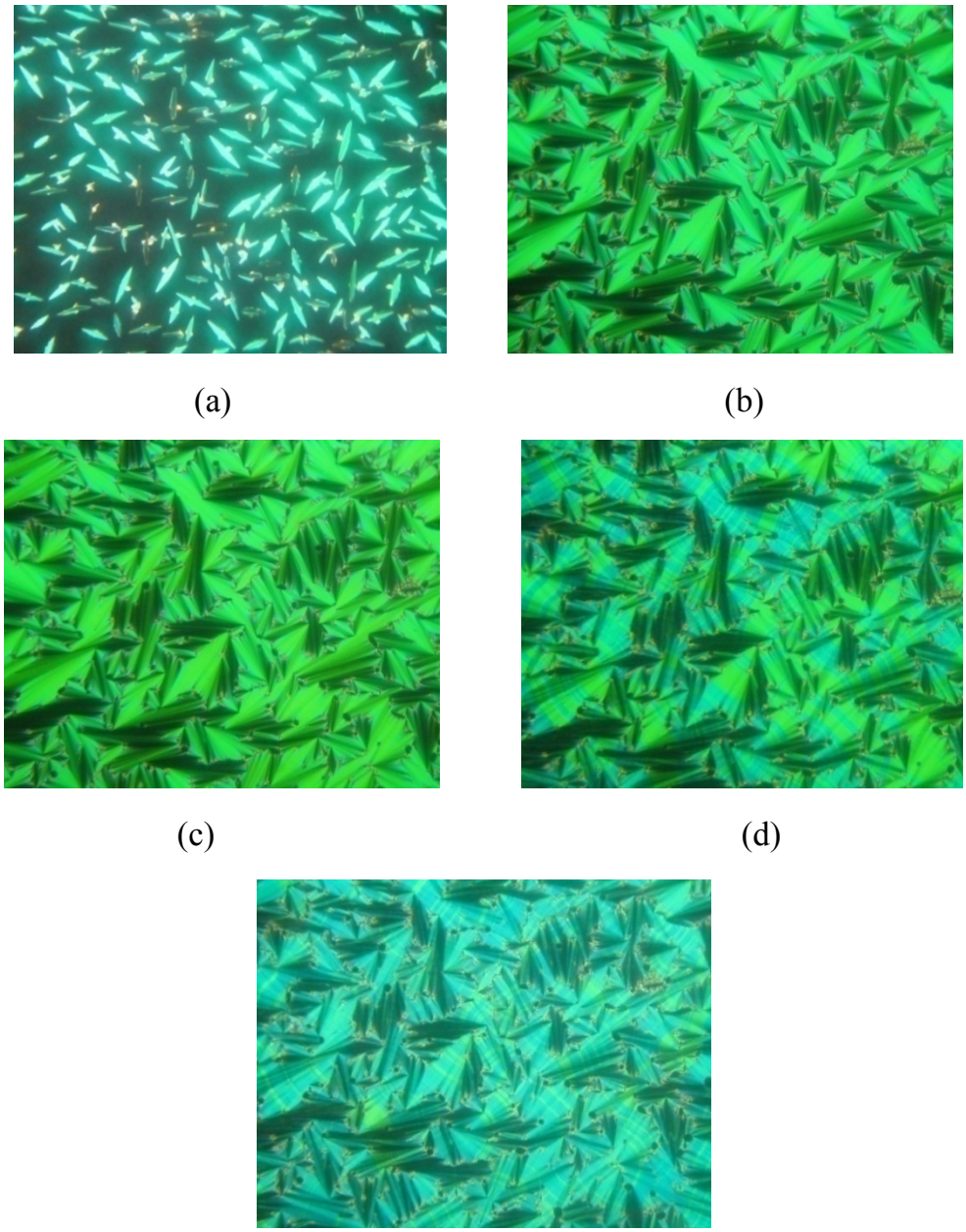

Figure 7.3. Photographs of the polarized optical microscopic textures for binary mixture with $x_{\text{comp.5}} = 0.1$ during cooling in: (a) Sm-*A* phase at 141.8 °C, (b) Sm-*A* phase at 129.7 °C, (c) Sm-*C** phase at 112.4 °C, (d) Sm-C_A* phase at 110.8 °C, (e) Sm-C_A* phase at 108 °C.

7.4. Spontaneous polarization measurements

The dynamics of the polarization switching behavior in both the Sm-*C** and Sm-C_A* phases has been investigated in 5 μm planar or homogeneously aligned (HG) cells using a square wave field. The time-dependent switching response for one of the mixtures ($x_{comp.5}$ = 0.2) at 93.5 °C is shown in figure 7.4 (V_{pp} = 38V, f = 20Hz). The extracted spontaneous polarization (P_s) values for the mixtures plotted as a function of reduced temperature (T/T_C) from the Curie point T_C (Sm-*C**–Sm-*A* transition) is shown in figure 7.5. The overall profile of the temperature dependence of P_s was found to be similar to that of pure chiral compound, i.e., (S)-MHPOBC [27]. Furthermore, the change in the P_s curve is subtle in going from the Sm-*C**–Sm-C_A* transition, suggesting a second order nature of that transition. All the mixtures were found to demonstrate relatively lower values of polarization than that of (S)-MHPOBC [27]. At a fixed T/T_C value, the spontaneous polarization assumes maximum value for the mixture comprising the highest share of the chiral component ($x_{comp.5}$ = 0.1), the obtained peak value being close to 110 nC cm^{-2} at T/T_C = 0.858. An enhancement in concentration of the achiral hockey stick-shaped molecule

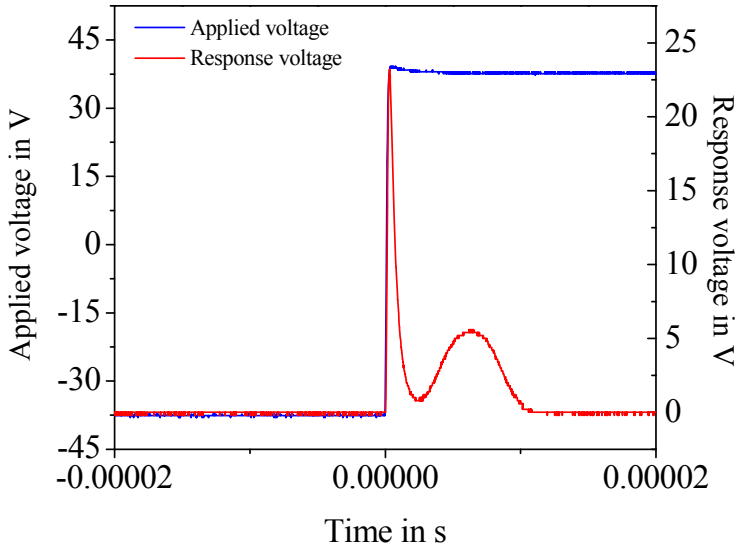

Figure 7.4. Switching voltage response observed in the Sm-C_A* phase of the mixture $x_{comp.5}$ = 0.2 at 93.5 °C under the applied square wave voltage.

causes a subsequent drop in polarization values. The mixture with $x_{comp.5} = 0.5$ has been found to possess the least P_s value at a specific reduced temperature with a maximum value of 28 nC cm^{-2} at $T/T_C = 0.974$. Such a concentration-dependent reduction is probably due to the dilatation effect of spontaneous polarization caused by addition of the achiral non-calamitic compound. Also, there may be a weakening of the core-core correlation among the molecules in these combined mesogenic systems [28–30]. The significant disparity in terminal chain length between the guest and host molecules also perhaps contributes to such decrease in P_s [31, 32].

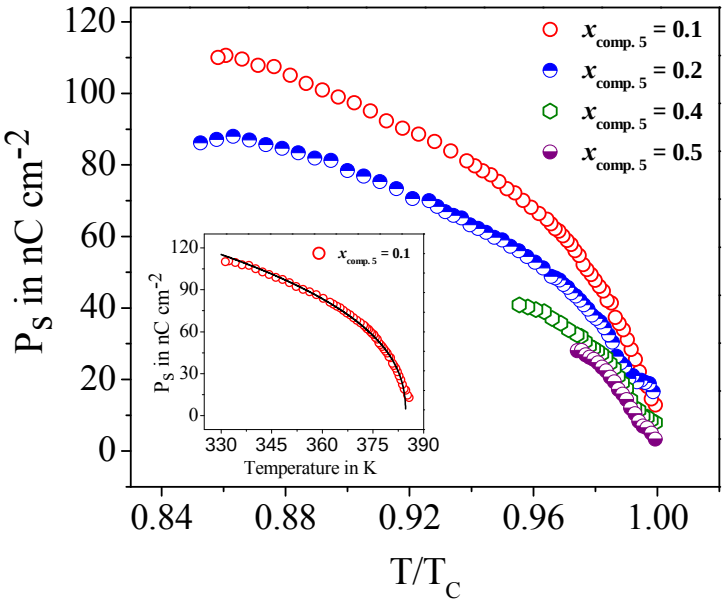

Figure 7.5. Spontaneous polarization (P_s) plotted as a function of reduced temperature for the four binary mixtures under investigation. Inset shows temperature dependence of P_s for the mixture with $x_{comp.5} = 0.1$. The solid line presents a fit to equation (7.1).

A plot of spontaneous polarization as a function of concentration of compound **5** at $T/T_C = 0.982$ is displayed in figure 7.6. Here, an extrapolation of the linear fit to the P_s values to $x_{comp.5} = 1$ yields a zero polarization value for the hockey stick-shaped molecule implying a non-polar character of the same. Such null outcome is in agreement with the result from direct measurement of

P_s for the investigated hockey stick-shaped compound using triangular wave voltage as described chapter 4.

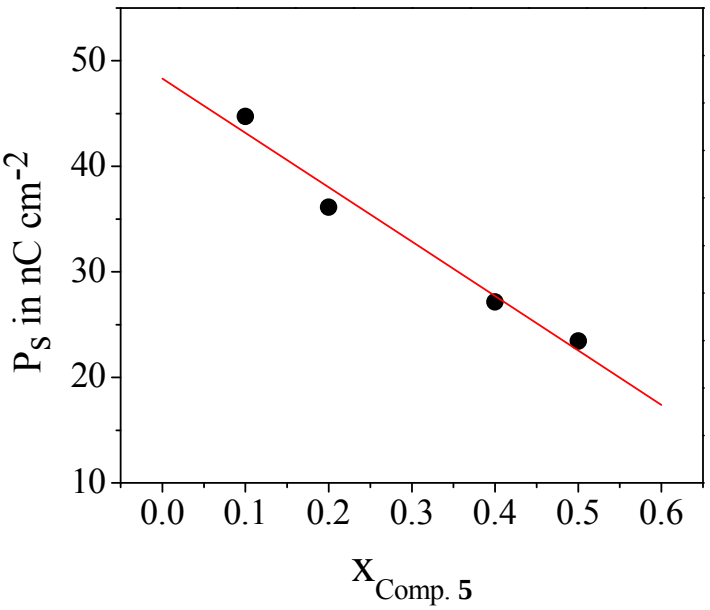

Figure 7.6. Spontaneous polarization (P_s) plotted as a function of concentration of compound **5** at $T/T_C = 0.982$ for the binary mixtures under investigation. The solid line is a linear fit to the data.

In an attempt to obtain an idea of the order-character of the Sm-*C**–Sm-*A* transition in the mixtures under investigation, the temperature dependence of P_s was fitted to the following expression [33],

$$P_s = P_0(T_c - T)^{\beta} \tag{7.1}$$

where, T_C is the Sm-*C**–Sm-*A* phase transition temperature, P_o and β are adjustable parameters. However, due to the limited availability of the P_s data, the above fit process cannot be accomplished for the two mixtures with higher fraction of the hockey stick-shaped compound, i.e., $x_{comp.5} = 0.4$ and 0.5. The measured P_s data were found to be well described by this equation for the remaining two mixtures (i.e., $x_{comp.5} = 0.1$ and 0.2). The yielded values of the fit parameters have been listed in table 7.1. Here, β values have been found to be 0.404 ± 0.006 and 0.384 ± 0.004 for mixtures with $x_{comp.5}$ = 0.1 and 0.2

respectively and hence, they are neither in agreement with the classical mean-field value, $\beta = 0.5$ nor with that expected for a tricritical system, i.e., $\beta = 0.25$ [34] and correspond to a second order nature of the ferroelectric–paraelectric transition in the mixtures under study.

Table 7.1. Values of the fit parameters obtained from the fit of the temperature dependence of P_s to equation (7.1).

$x_{comp.5}$	P_0 in nC cm^{-2}	T_c in K	β
0.1	22.9 ± 0. 5	384.7 ± 0. 1	0.404 ± 0.006
0.2	20.0 ± 0.3	377.2 ± 0.1	0.384 ± 0.004

7.5. Response time and effective torsional bulk viscosity measurements

Figure 7.7 depicts the reduced temperature dependent variation of the response time (τ) for the mixtures under study. At a specific reduced temperature, the τ values are observed to be enhanced monotonically with increase in concentration of the hockey stick-shaped compound. The magnitudes of response time for the two mixtures with relatively lower concentration of hockey stick-shaped molecules, i.e., $x_{comp.5} = 0.1$ and 0.2 are found to be always higher than that of the other two mixtures over their entire mesogenic range. However, the difference in τ values among all the mixtures is not more than 3–4.5 μs at a fixed T/T_C value. The maximum values of the response time are observed to be in the range between 6 and 27 μs for the different mixtures. At a specific reduced temperature, τ values are found to be minimum for the mixture with $x_{comp.5} = 0.1$ and maximum for that with $x_{comp.5} = 0.5$.

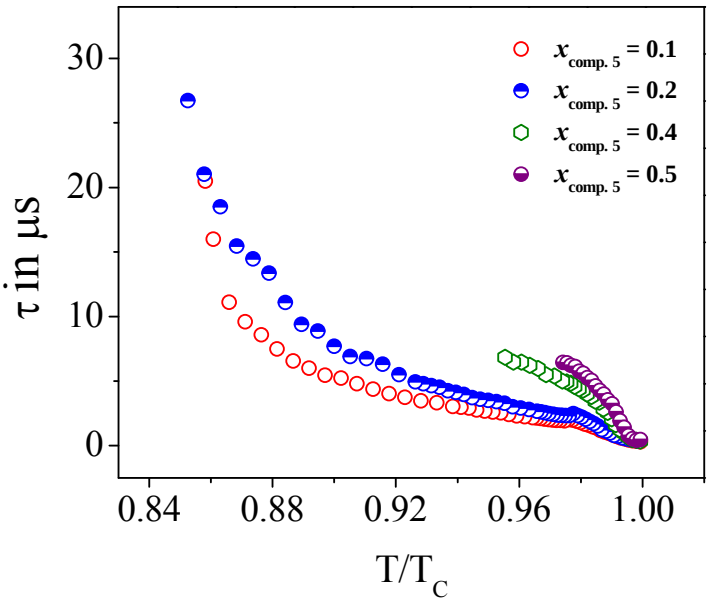

Figure 7.7. Response time (τ) plotted as a function of reduced temperature for the four binary mixtures under investigation.

The effective torsional bulk viscosity (η), which is related to the molecular reorientation around the Sm-*C** cone and decides the switching time of the director, is one of the most crucial parameters in describing the dynamics of chiral molecules. For the binary mixtures under investigation, the variation of η against T/T_C is illustrated in figure 7.8. The magnitudes of the torsional viscosity coefficient for the mixtures with $x_{\text{comp.5}}$ = 0.1 and 0.2 have been observed to be close to one another over a wide range of temperature (up to $T/T_C \sim 0.92$). Notably, at a specific reduced temperature, the remaining two mixtures also exhibit no significant deviation in η values from those of the other members of this binary system. Such a reluctant concentration dependence of η is also in agreement with subtle variation of τ on the concentration scale. This trivial variation in torsional viscosity coefficient and the related relaxation time may be accounted for qualitatively on the basis of the Boulder model [35, 36]. According to this model, in the combined mesogenic medium, the chiral molecues causes a modification in the orientational distributions of the transverse dipole momemt of achiral

molecules with regard to the polar C_2 axis. Now, depending on the structural resemblance of the chiral and achiral components present in the mixture, such interactions via core-core interactions may either favor or oppose orientations of the transverse dipole moment along the polar C_2 axis [28]. In this case, probably such effect of redistributing the component of transverse dipole moment is relatively less effective (i.e., less chiral perturbation) in redefining the distribution of dipolar contribution from the achiral bent-mesogenic molecules in the association.

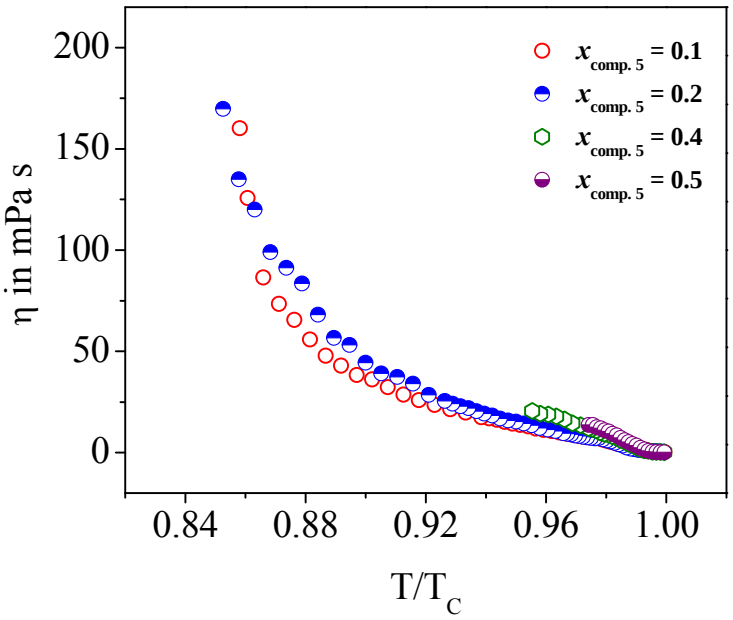

Figure 7.8. Effective torsional bulk viscosity (η) plotted as a function of reduced temperature for the four binary mixtures under investigation.

In an attempt to obtain knowledge of the associated activation energy (E_a) related to the reorientation of molecule on the cone of reversal of the applied field, the temperature dependence of η was fitted with the following expression [37]:

$$\eta = \eta_0 \, exp\left(\frac{E_a}{k_\beta T}\right) \tag{7.2}$$

where k_β is the Boltzmann's constant and T is the temperature on absolute scale. The Arrhenius plot of the effective torsional bulk viscosity for two binary mixtures with $x_{comp.5} = 0.1$ and 0.2 are illustrated in figure 7.9. The slope of the linear region in those plots, far away from transition, can be utilized to evaluate the E_a values. Activation energy has been found to be about 0.58 eV and 0.65 eV for mixtures with $x_{comp.5} = 0.1$ and 0.2 respectively. However, due to the relatively smaller width of the chiral smectic phase, it was not possible to measure the E_a values with the desired degree of accuracy for mixtures with $x_{comp.5} = 0.4$ and 0.5 due to an inadequate number of data points. The obtained E_a values are again relatively higher than those reported by others for dissimilar mesogenic systems [37].

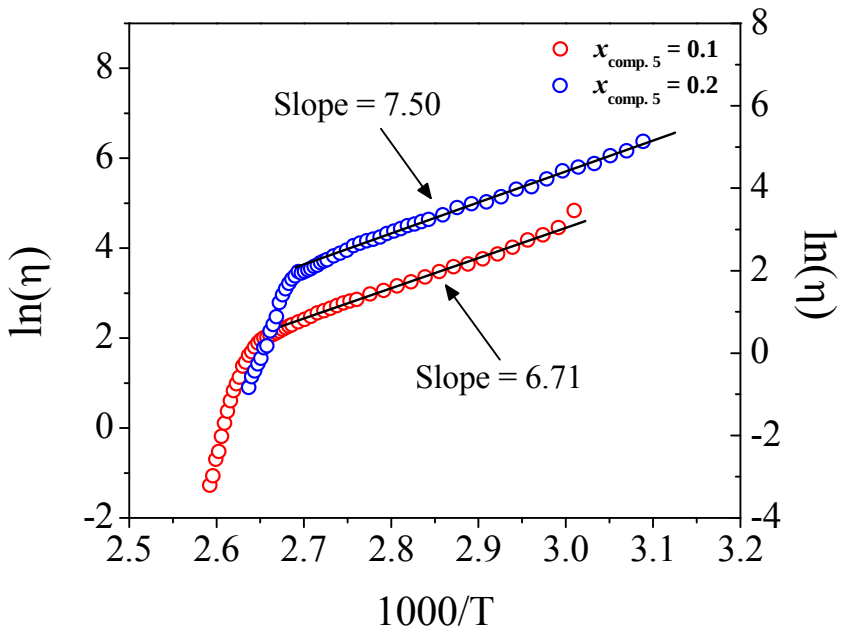

Figure 7.9. Logarithmic plot of effective torsional bulk viscosity versus (1000/T) for mixtures with $x_{comp.5} = 0.1$ and 0.2. Solid line (—) represents best fit of the data to equation (7.2).

7.6. Anchoring strength coefficient measurements

The anchoring energy coefficient gives a quantitative description of the strength of alignment of liquid crystal molecules relative to cell-substrate.

Depending on the nature of interactions between the molecules of liquid crystals and those in the aligning layer, these coefficients can be categorized as (i) the dispersion anchoring energy coefficient (W_D) (related to the non-electrostatic interaction among the molecules, i.e., those due to the dispersion or van der Waals forces) and (ii) polarization anchoring energy coefficient (W_P) (related to the electrostatic part of interaction) [38–41]. In this study, magnitude of both the dispersion anchoring strength coefficient and polarization anchoring strength coefficient have been determined at different temperature using the following equations [38–41]

$$W_D = \frac{\eta d}{4\tau} \tag{7.3}$$

and

$$W_P = \sqrt{P_s \sqrt{W_D}} \tag{7.4}$$

Variations of W_D and W_P as a function of reduced temperature are shown in figures 7.10 and 7.11 respectively.

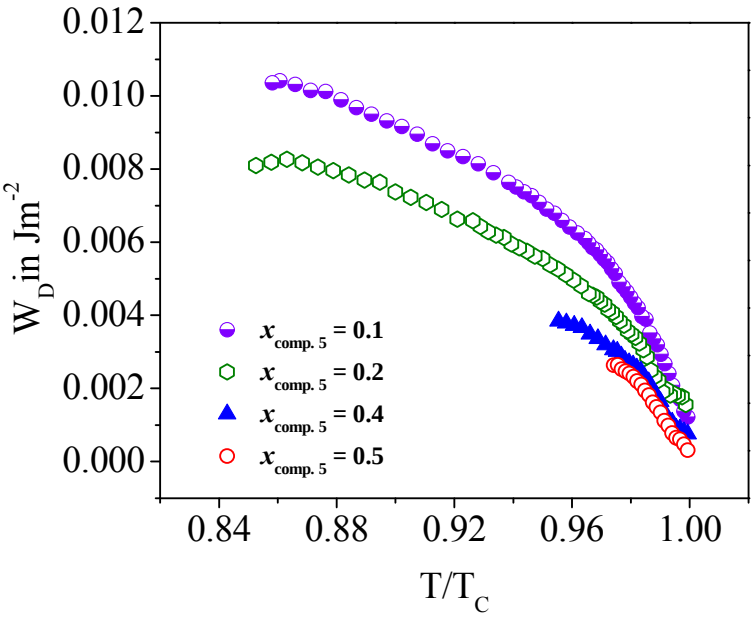

Figure 7.10. Dispersion anchoring energy coefficient (W_D) plotted as a function of reduced temperature for the four binary mixtures under investigation.

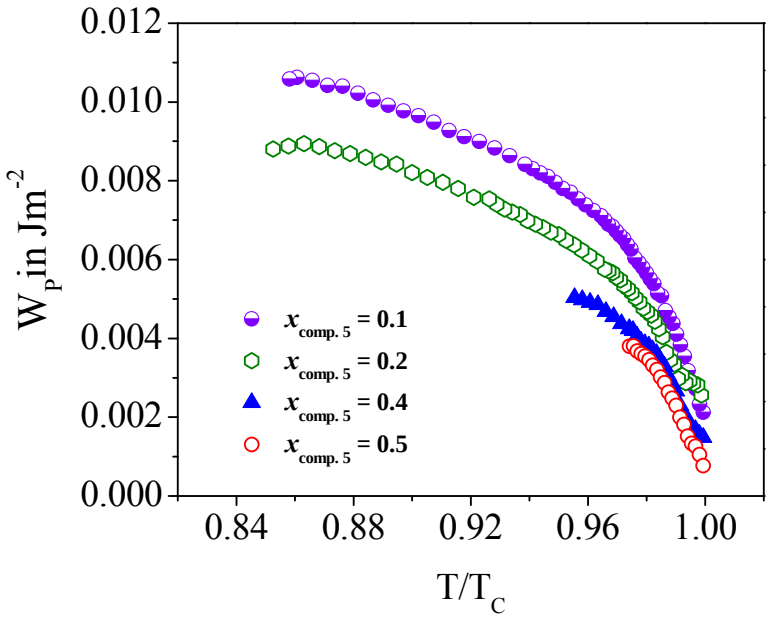

Figure 7.11. Polarization anchoring energy coefficient (W_P) plotted as a function of reduced temperature for the four binary mixtures under investigation.

The overall shape of the reduced temperature dependences of both W_D and W_P are as expected, wherein they exhibit a decreasing trend with enhancement in temperature towards the Sm-*C**–Sm-*A* transition. Such a behavior is due to the fact that an enhancement in temperature causes a related augmentation in enthalpy of the concerned mesogenic medium which eventually leads to a breaking of their interaction barrier [42]. Furthermore, at a fixed reduced temperature, both of W_D and W_P are found to be diminished continually with increase in concentration of the hockey stick-shaped compound, being least for the mixture with $x_{\text{comp.5}}$ = 0.5. An inspection of figure 7.10 also reveals that in the neighborhood of the Sm-*C**–Sm-*A* transition, the W_D values are nearly proportional to the T/T_C values. Such observation again is in agreement with those reported by others [38]. Moreover, from the plot displaying the variation of W_D against W_P (figure 7.12), it is apparent that for all of the mixtures at a particular temperature, the

magnitude of two anchoring energy coefficient are nearly identical suggesting equal contribution from the polar and non-polar parts of interaction.

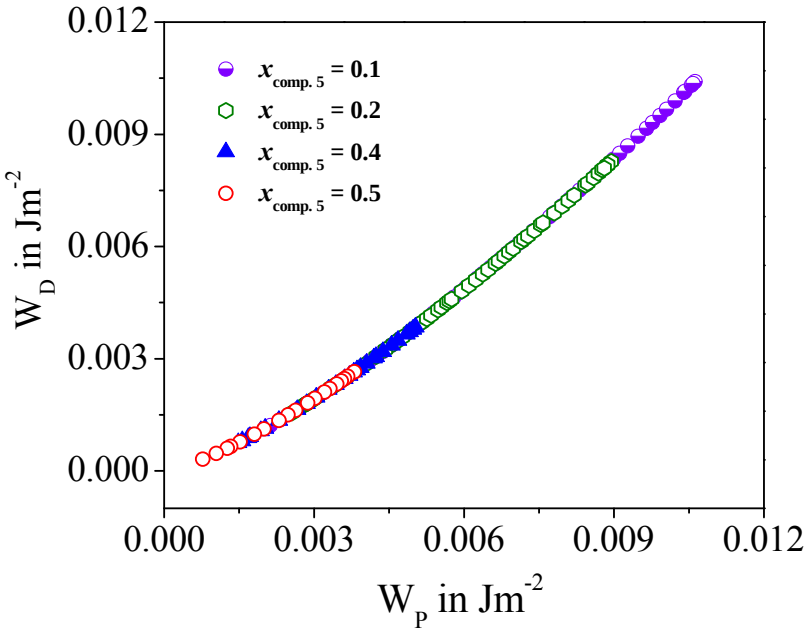

Figure 7.12. Plot of dispersion anchoring energy coefficient (W_D) as a function of polarization anchoring energy coefficient (W_P) for the four binary mixtures under investigation.

7.7. Conclusions

Electro-optical measurements have been carried out in the mesophases of a few binary liquid crystal mixtures, comprising an achiral hockey stick-shaped compound and the chiral (S)-MHPOBC. In these mixtures, the spontaneous polarization has been found to be significantly influenced by the addition of bent-mesogenic molecules in chiral environment where an enhancement in concentration of the hockey stick-shaped molecules causes a significant reduction in P_s. An extrapolation of the linear fit to the P_s values yields a zero polarization value for the investigated hockey stick-shaped compound, confirming the non-polar character of the same. Interestingly, the response time and effective torsional bulk viscosity coefficient are found to demonstrate a feeble dependence on achiral compound concentration and

assume values close to 2–10 μs and 10–50 mPa s respectively, over a wide range of temperature in the mesophases. Such an outcome is conceivably due to the weak perturbation, experienced by the hockey stick-shaped molecules in the chiral environment. Moreover, for a specific mixture, resemblance in magnitudes of the dispersion and polarization anchoring strength coefficients indicates nearly equal share in anchoring energy from electrostatic and non-electrostatic parts of interaction. Hence, the considered asymmetric bent-shaped molecules induce a considerable reduction in magnitude of spontaneous polarization and hence, a related elongation of the helix [as the pitch of the helix has found to be approximately inversely proportional to spontaneous polarization (43)] in the investigated antiferroelectric system without affecting the molecular relaxation time considerably. Even though a number of issues need to be resolved, such chiral–achiral mixtures involving bent-structures may prove to be a viable route for designing materials with potential for different electro-optic applications, especially where low polarization and long pitch are required.

References:

[1] T. Niori, T. Sekine, J. Watanabe, T. Furukawa, and H. Takezoe, *J. Mater. Chem.*, **6**, 1231 (1996).

[2] G. Pelzl, S. Diele, and W. Weissflog, *Adv. Mater.*, **11**, 707 (1999).

[3] H. Takezoe and Y. Takanishi, *Jpn. J. Appl. Phys.*, **45**, 597 (2006).

[4] R. Amaranatha Reddy and C. Tschierske, *J. Mater. Chem.*, **16**, 907 (2006).

[5] S. Diele, S. Grande, H. Kruth, Ch. Lischka, G. Pelzl, W. Weissflog and I. Wirth, *Ferroelectrics*, **212,** 169 (1998).

[6] D. R. Link, G. Natale, R. Shao, J. E. Maclennan, N. A. Clark, E. Körblova, and D. M. Walba, *Science*, **278**, 1924 (1997).

[7] D. M. Walba, D. J. Dyer, T. Sierra, P. L. Cobben, R. Shao, and N. A. Clark, *J. Am. Chem. Soc.*, **118**, 1211 (1996).

[8] M. Hird, *Liq. Cryst. Today*, **14**, 9 (2005).

[9] S. Findeisen-Tandel, M. W. Schröder, G. Pelzl, U. Baumeister, W. Weissflog, S. Stern, A. Nemes, R. Stannarius, and A. Eremin, *Eur. Phys. J. E*, **25**, 395 (2008).

[10] D. Chen, Y. Shen, C. Zhu, L. E. Hough, N. Gimeno, M. A. Glaser, J. E. Maclennan, M. B. Ros, and N. A. Clark, *Soft Matter*, **7**, 1879 (2011).

[11] J. Harden, B. Mbanga, N. Éber, K. Fodor-Csorba, S. Sprunt, J. T. Gleeson, and A. Jákli, *Phys. Rev. Lett.*, **97**, 157802 (2006).

[12] J. Harden, R. Teeling, J. T. Gleeson, S. Sprunt, and A. Jákli, *Phys. Rev. E*, **78**, 031702 (2008).

[13] D. Wiant, J. T. Gleeson, N. Éber, K. Fodor-Csorba, A. Jákli, and T. Tóth-Katona, *Phys. Rev. E*, **72**, 041712 (2005).

[14] S. Tanaka, S. Dhara, B. K. Sadashiva, Y. Shimbo, Y. Takanishi, F. Araoka, K. Ishikawa, and H. Takezoe, *Phys. Rev. E*, **77**, 041708 (2008).

[15] S. Tanaka, H. Takezoe, N. Éber, K. Fodor-Csorba, A. Vajda, and A. Buka, *Phys. Rev. E*, **80**, 021702 (2009).

[16] S. Dhara, F. Araoka, M. Lee, K. V. Le, L. Guo, B. K. Sadashiva, K. Song, K. Ishikawa, and H. Takezoe, *Phys. Rev. E*, **78**, 050701 (2008).

[17] C. Bailey, K. Fodor-Csorba, J. T. Gleeson, S. N. Sprunt, and A. Jákli, *Soft Matter*, **5**, 3618 (2009).

[18] E. Dorjgotov, K. Fodor-Csorba, J. T. Gleeson, S. Sprunt, and A. Jákli, *Liq. Cryst.*, **35**, 149 (2008).

[19] R. Cristiano, A. A. Vieira, F. Ely, and H. Gallardo, *Liq. Cryst.*, **33**, 381 (2006).

[20] V. Novotná, J. Žurek, V. Kozmík, J. Svoboda, M. Glogarová, J. Kroupa, and D. Pociecha, *Liq. Cryst.*, **35**, 1023 (2008).

[21] S. Radhika, H. T. Srinivasa, and B. K. Sadashiva, *Liq. Cryst.*, **38**, 785 (2011).

[22] P. Sathyanarayana, S. Radhika, B. K. Sadashiva, and S. Dhara, *Soft Matter*, **8**, 2322 (2012).

[23] F. C. Yu and L. J. Yu, *Chem. Mater*., **18**, 5410 (2006).

[24] F. C. Yu and L. J. Yu, *Liq. Cryst*., **35**, 799 (2008).

[25] R. Stannarius, J. Li, and W. Weissflog, *Phys. Rev Lett*., **90**, 025502 (2003).

[26] M. Glogarová , H. Sverenyák , A. Fukuda, and H. Takezoe, *Liq. Cryst.*, **14**, 463 (1993).

[27] A. Pramanik, M. K. Das, B. Das, M. Żurowska, and R. Dabrowski, *Liq. Cryst.*, **42**, 412 (2015).

[28] R. P. Lemieux, *Chem. Soc. Rev*., **36**, 2033 (2007).

[29] R. P. Lemieux, *Acc. Chem. Res.*, **34**, 845 (2001).

[30] D. Vizitiu, C. Lazar, B. J. Halden, and R. P. Lemieux, *J. Am. Chem. Soc.*, **121**, 8229 (1999).

[31] S. Jaradat, N. W. Roberts, Y. Wang, L. S, Hirst, and H. F. Gleeson, *J. Mater. Chem.*, **16**, 3753 (2006).

[32] M. P. Thompson, and R. P. Lemieux, *J. Mater. Chem.*, **17**, 5068 (2007).

[33] A. D. L. Chandani, T. Hagiwara, Y. Suzuki, Y. Ouchi, H. Takezoe, and A. Fukuda, *Jpn. J. Appl. Phys*., **27**, L729 (1988).

[34] H. Yurtseven and D. Kavruk, *Ferroelectrics*, **367**, 190 (2008).

[35] D. M. Walba, *Advances in the Synthesis and Reactivity of Solids*, T. E. Mallouk (Ed.), **Vol. 1**, JAI Press Ltd, Greenwich (1991).

[36] D. M. Walba and N. A. Clark, *Proc. SPIE, Spatial Light Modulators and Applications II*, **0825**, 81 (1988).

[37] J. Hemine, A. Daoudi, M. Zazoui, C. Legrand, N. Isaert, A. Elkaaouachi, and H. T. Nguyen, *Spectrosc. Lett.*, **41**, 285 (2008).

[38] L. M. Blinov and V. G. Chigrinov, *Electrooptic Effects in Liquid Crystal Materials*, Springer-Verlag, New York (1994).

[39] A. I. Allagulov, S. A. Pikin, and V. G. Chigrinov, *Liq. Cryst.*, **5**, 1099 (1989).

[40] J. F. Lyuu, C. C. Chen, and J. Y. Lee, *Mol. Cryst. Liq. Cryst.*, **329**, 99 (1999).

[41] A. K. Misra, A. K. Srivastava, J. P. Sukla, and R. Manohar, *Phys. Scr.*, **78**, 065602 (2008).

[42] S. S. Seomun, B. Park, A. D. L. Chandani, D. S. Herman, Y. Takanishi, K. Ishikawa, H. Takezoe, and A. Fukuda, *Jpn. J. Appl. Phys.*, **36**, 3586 (1997).

[43] A. Lapanik, A. Rudzki, B. Kinkead, H. Qi, T. Hegmann, and W. Haase, *Soft Matter*, **8**, 8722 (2012).